

---

# In Vitro Evaluation

---

---

## INITIAL IN VITRO INTERACTION OF HUMAN OSTEOBLASTS WITH NANOSTRUCTURED HYDROXYAPATITE (NHA)

XINGYUAN GUO<sup>1</sup>, JULIE GOUGH<sup>1</sup>, PING XIAO<sup>1</sup>

1. Manchester Materials Science Centre, School of Materials, The University of Manchester,  
Grosvenor street, Manchester, UK, M1 7AZ

JING LIU<sup>2</sup> ZHIJIAN SHEN<sup>2</sup>

2. Department of Inorganic Chemistry, Arrhenius Laboratory, Stockholm University, S-  
10691, Stockholm, Sweden

### ABSTRACT

Nanostructured hydroxyapatite (NHA) was fabricated by Spark Plasma Sintering (SPS), while microstructured hydroxyapatite (MHA) by conventional method. Human Osteoblasts were cultured on both NHA and MHA and the cell attachment, proliferation and mineralisation were evaluated. After 90 min incubation the cell density on NHA surface is significantly higher than that of MHA and glass control, whereas average cell area of a spread cell is significantly lower on NHA surface compared to MHA and glass control after 4 h incubation. Mineralisation of matrix has been determined after 14 days culture by using alizarin red assay combined with cetylpyridinium chloride (CPC) extraction. NHA shows significant enhancement ( $p < 0.05$ ) in mineralisation compared to MHA. Results from this study suggest that NHA is a much better candidate for clinical uses in terms of bioactivity.

### 1. INTRODUCTION

Interaction between cells and implanted materials depends on the physical and chemical characteristics of materials and particularly on its chemical composition, particle size and surface properties, which include their topography, roughness, surface energy, hydrophilicity and hydrophobicity<sup>1-3</sup>. Such characteristics determine how biological molecules will adsorb to the surface. Specifically, maximum vitronectin (a protein contained in serum that is known to mediate osteoblast adhesion<sup>4</sup>), fibronectin and albumin adsorption was noted on hydrophilic surface with high surface roughness and /or energies, such selected protein has been identified to mediate adhesion of specific anchorage-dependent cells (such as osteoblasts, fibroblasts, and endothelial cells) on substrate surfaces<sup>5</sup>. Therefore, surface properties will affect cell adhesion, attachment on implanted materials in the first phase of cell/material interactions and thus further influence the cell's capacity to proliferate and to differentiate on contact with the implant<sup>2, 6</sup>. Design of materials with improved physical and chemical properties could enhance cell response to biomaterial implants and further extend their lifetime and, therefore, decrease the rate of revision surgery.

It has been reported that surface properties (such as surface area, charge, and topography) depend on the grain size of a material.<sup>5</sup> In this respect, nanostructured materials possess higher surface area with increased portions of surface defects and grain-boundaries.<sup>7</sup> Meanwhile, hydroxyapatite has been considered as a good candidate for designing hard tissue implants due to its excellent biological properties such as non-toxicity, lack of inflammatory response and immunological reactions, and is able to intimately bond to new bone<sup>8, 9</sup>. Consequently, It is extremely attractive to explore if and how nanostructured hydroxyapatite with enhanced surface properties (such as increased surface area and charge, as well as ability to alter adsorption of

chemical species) could be used to promote cell response and bonding of juxtaposed bone to an orthopaedic or dental implants composed of nanophase ceramics. However, only a few reports have been published till now. Webster has reported that osteoblasts adhesion and osteoblasts proliferation was significantly greater on nanophase alumina, titania, and hydroxyapatite than on conventional formulations of the same ceramic after 3 and 5 days and more importantly, compared to conventional ceramics, synthesis of alkaline phosphatase and deposition of calcium containing mineral was significantly greater by osteoblasts cultured on nanophase than conventional ceramics after 21 days and 28 days.<sup>5, 10, 11</sup> In this article, a primary human osteoblast cell model has been used to study the cellular response to nanostructured HA (NHA) compared with microstructured HA (MHA).

## 2 EXPERIMENTS

### 2.1 Materials

HA powder has been prepared by precipitation at room temperature using  $\text{Ca}(\text{OH})_2$  and  $\text{H}_3\text{PO}_4$  as starting materials<sup>12</sup>. Such powder has been characterized using XRD and FTIR as a hydroxyapatite phase with low crystallinity and with incorporation of carbonate ions. The shape of the HA crystals are acicular according to TEM images. Crystallite size calculated according to XRD results is about 20-40 nm, while the particle size measured by Mastersizer microplus (Malvern Ltd, UK) is several microns. All nanostructured HA (NHA) samples used for cell culture were sintered at 900°C for 3 min by the SPS process with a heating rate of  $100^\circ\text{C}\cdot\text{min}^{-1}$  and a pressure of 50 MPa at vacuum atmosphere. All microstructured HA (MHA) compacts were sintered by conventional method at 1200°C for 2 h with a heating rate of  $5^\circ\text{C}\cdot\text{min}^{-1}$  in air.

### 2.2 Surface characterisation

The sintered compacts were polished using Silica colloid ( $0.06\mu\text{m}$ ) and chemically etched in 18.0 mM HCl solution to reveal the grain boundaries, and then microstructural observations of sintered ceramics were conducted using a high-resolution scanning electron microscope (FESEM-XL30, Philips). Topography and surface roughness of NHA and MHA has been evaluated by Atomic force microscopy (AFM). Five measurements were made on each sample with a scanning area of  $5 \times 5 \mu\text{m}$ . The classical mean surface roughness parameter  $R_a$  has been used to characterize surface roughness. Aqueous wettability of nanostructured HA and microstructured HA has been analysed by contact angle measurements on polished samples. Measurements were run in triplicate per sample and repeated at three different times.

### 2.3 Cell morphology

HOBs in complete Dulbecco's modified Eagles medium (DMEM) containing 10% foetal bovine serum (FBS), 1% antibiotics and 0.85mM ascorbic acid-2 phosphate were seeded onto microstructured HA (MHA) and nanostructured HA (NHA) discs at a density of  $4 \times 10^4$  cells/cm<sup>2</sup>, then incubated at 37°C in a humidified incubator with 5% CO<sub>2</sub> for 90 min, 4 h, and 24 h. Glass coverslips purchased from Chance Glass Ltd were used as control materials. At the pre-determined time points, samples were rinsed in phosphate buffered saline (PBS) to remove any non-adherent cells and medium. The remaining cells were fixed in 1.5% glutaraldehyde for 30 min at 4°C, then dehydrated through a series of ethanol concentrations (50%, 70%, 90%, and 100%) and dried using hexamethyldisilazane (HMDS). Once dry, the samples were coated with gold and examined in a JEOL JSM-840 Scanning Electron Microscope at 10kV<sup>13, 14</sup>.

#### 2.4 Cell proliferation

Cells were harvested with 0.1% trypsin-EDTA solution in phosphate-buffered saline (PBS, pH 7.4) from cell culture flasks and were resuspended in culture medium, then were seeded at a concentration of  $4 \times 10^4$  cells/cm<sup>2</sup> onto disks of MHA and NHA. Tissue culture polystyrene was used as a control material. Cells were left to grow on the disks for 1, 3, 7 days in a 37°C incubator with 5% CO<sub>2</sub>. At the pre-determined time points, each of the disks was transferred to new wells in a new 24-well plate and 1.5 ml medium were added to each disk. 150 µl of freshly prepared 5 mg/ml 3-(4,5-dimethylthiazolyl-2)-2,5-diphenyltetrazolium bromide (MTT) were added to each well containing the disks. The plates were placed in an incubator at 37°C for 3 h. Afterwards, the supernatant of each well were removed and acidified isopropanol (0.04 M HCl in isopropanol) was added to all wells and mixed thoroughly to dissolve the dark-blue crystals. After all crystals were dissolved, the plates were read on a Microplate reader (Ascent) with a test wavelength of 540 nm against a reference wavelength of 620 nm<sup>15</sup>.

#### 2.5 Alamar Blue™ assay

Cells were harvested with 0.1% trypsin-EDTA solution in phosphate-buffered saline (PBS, pH 7.4) from cell culture flasks and were resuspended in culture medium, then were seeded at a concentration of  $4 \times 10^4$  cells/cm<sup>2</sup> onto disks of MHA and NHA. Tissue culture polystyrene was used as a control material. After 1 day incubation in a 37°C incubator with 5% CO<sub>2</sub>, samples were taken out into new wells and 1.25 µg/ml Alamar Blue™ were added into each well, then incubated for 3 h. The fluorescence was measured using a FLUOstar OPTIMA (BMG LABTECH) plate reader at 530ex-590em nm wavelengths. The suspension containing Alamar Blue™ was removed from sample wells and new medium added to incubate further<sup>16,17</sup>.

#### 2.6 Mineralisation

Ability of cells to produce mineralised matrix is essential with regard to development of materials for bone regeneration. Whether mineralisation of matrix occurred was determined using alizarin red-S (AR-S) assay combined with cetylpyridinium chloride (CPC) extraction<sup>18,19</sup>. Alizarin red is a dye which binds selectively to calcium salts and is widely used for calcium mineral histochemistry. AR-S binds ~2 mol of Ca<sup>2+</sup> /mol of dye in solution. Briefly, Cells were seeded onto disks of MHA and NHA at a concentration of  $4 \times 10^4$  cells/cm<sup>2</sup> by using medium, which was supplemented with 10 mM β-glycerophosphate and 100 nM dexamethasone. Tissue culture polystyrene was used as a control material. At the pre-determined time points (7,14 days), samples were briefly rinsed with PBS followed by fixation (ice-cold 70% ethanol, 1 h). Samples then were rinsed with nanopure water and stained for 10 min with 40 mM AR-S, pH 4.2, at room temperature. Afterwards, samples were rinsed five times with water followed by a 15 min wash with PBS to reduce non-specific AR-S stain. Stained cultures were destained by using 10% (w/v) cetylpyridinium chloride (CPC) in 10 mM sodium phosphate, pH 7.0, for 15 min at room temperature. After destain, the plates were read on a Microplate reader (Ascent) with a test wavelength of 540 nm against a reference wavelength of 620 nm. Furthermore, for determination of the matrix mineralisation directly on HA samples, two groups of samples were used. Group 1 was cultured with HOBs, and Group 2 without HOBs as background. To calculate the mineral content of the extracellular matrix, group 2 values were subtracted from group 1.

#### 2.7 Statistical analysis

All samples were run in triplicate and repeated three times. Statistical analysis was performed using student's t-test, and a p value of <0.05 was determined to represent a significant difference.

### 3 RESULTS

Fig.1 shows the scanning electronic microstructure of NHA and MHA. Dense compact consisting of equiaxed grains with an average grain size of ~90 nm was obtained by SPS (as shown in Fig. 1A), whereas the grain size is about 2  $\mu\text{m}$  when sintering by conventional method at 1200°C as shown in Fig. 1B. The relative density of NHA is 100%, whereas 95% of MHA measured by Archimedes method with deionized water as the immersion medium. After sintering, NHA was characterized as pure HA with nanostructured feature, while MHA was characterized with slightly decomposition to tetracalcium phosphate (results not shown in this article).

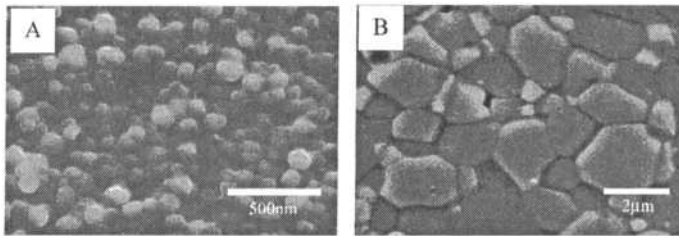


Fig.1 SEM morphologies of (A) NHA and (B) MHA

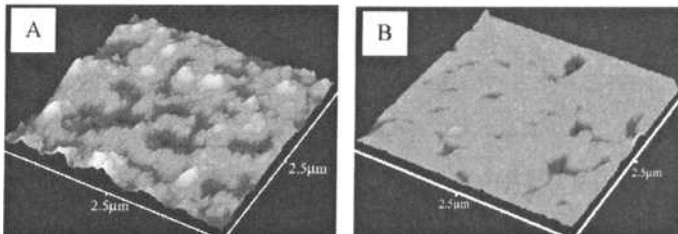


Fig.2 Topography of (A) NHA and (B) MHA

According to contact angle measurement, aqueous contact angle on NHA is 30°, whereas 42° on MHA, which was significantly ( $p < 0.05$ ) higher than that on NHA. The decrease in contact angle corresponds to an increase in surface aqueous Wettability and, thus, an increase in hydrophilicity and surface reactivity for NHA. Topography measured by Atomic force microscopy (AFM) presents in Fig.2 shows that surface of MHA is much smoother than that of NHA. Surface roughness calculated from AFM data provided evidence that NHA possesses significantly higher roughness ( $37.2 \pm 5.5 \text{ nm}$ ) compared to MHA ( $12.1 \pm 3.0 \text{ nm}$ ).

Fig. 3 shows the SEM morphologies of human osteoblasts cultured on NHA and MHA after 90 min, 4 h, and 24 h with glass as control material. Different morphologies have been observed on various surfaces. At 90 min most cells present a spherical, spiky appearance on both HA surfaces, whereas more spread cells are observed on glass. Abundant filopodia were visible

Initial in Vitro Interaction of Human Osteoblasts with Nanostructured Hydroxyapatite (HNA)

at the edge of cells on both HA surfaces, in particular on the NHA surface. Those spiky and more three-dimensional morphologies of cells cultured on HA surfaces might be attributed to surface

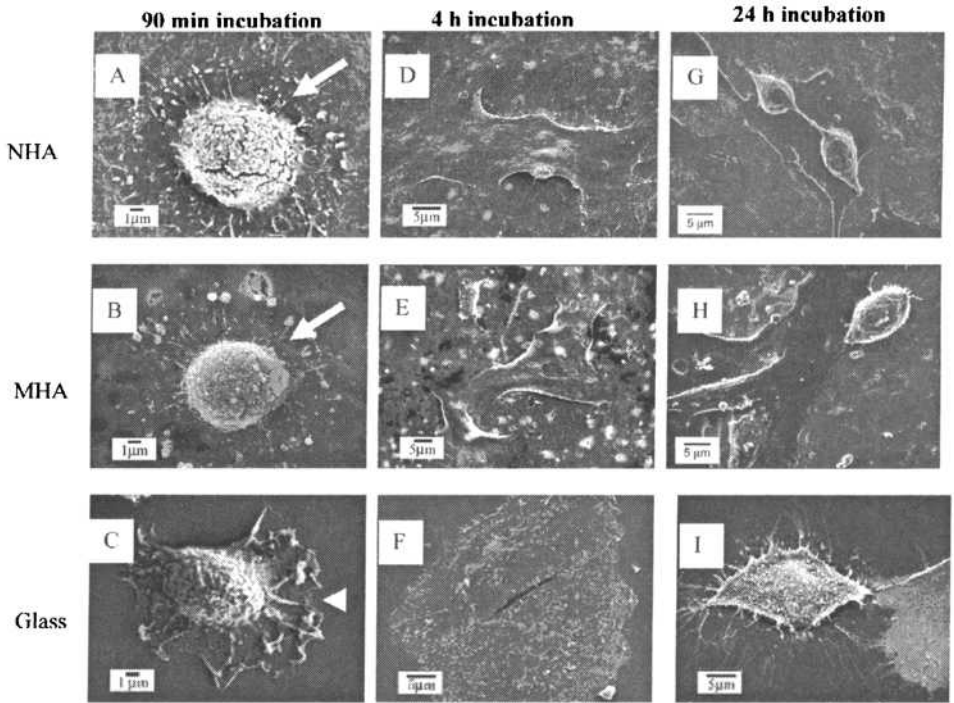


Fig.3 SEM micrographs of osteoblasts cultured for 90 min (A-C), 4 h (D-F), 24 h (G-I) on the surface of NHA, MHA and glass control respectively. Arrow indicates filopodia. arrowhead indicates ruffles.

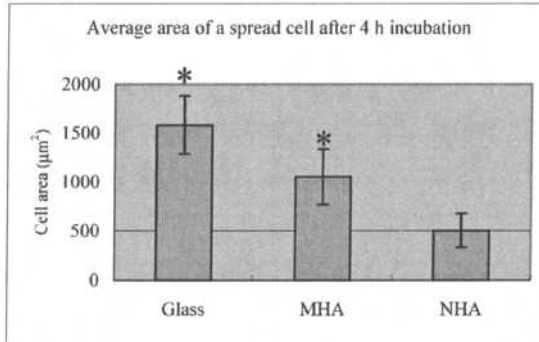


Fig. 4 Cell density on NHA, MHA and Glass after 90 min incubation, \* significantly higher than MHA and Glass ( $p < 0.05$ ,  $n = 5$ ) roughness.<sup>14</sup> After 4 h incubation, cells spread on all surfaces with the edge of the cells becoming very thin. At 24 h, cells became thicker at the center of nucleus, and mitosis was evident on some surfaces.

The cell density on both HA samples and Glass sample after 90 min incubation has been measured by counting cells in 5 randomly selected areas under SEM with a magnification of 200, results of which is shown in Fig. 4. The cell density on NHA is significantly higher compared to that on MHA and glass, which suggested that nanostructured surface promote osteoblast adhesion in the first stage. The average areas of spread cells on various samples after 4 h incubation were measured by image analysis software (UTHSCSA Image Tool) from 20 randomly selected cells, which is shown in Fig. 5. The results indicated that cell spread significantly widely on both glass and microstructured HA compared to nanostructured HA.

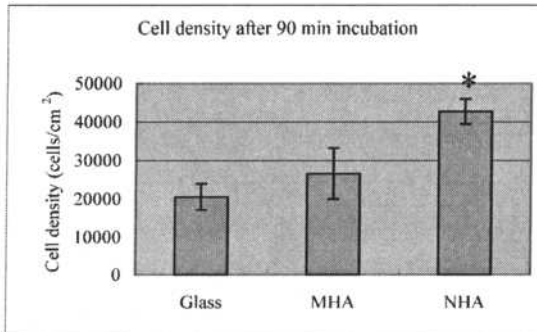


Fig. 5 The average area for a spread cell on various samples after 4 h incubation, 20 cells were measured from 5 randomly selected areas of each sample, and average area was calculated from the measurements. \* Significant from NHA ( $p < 0.05$ ,  $n = 20$ )

## Initial in Vitro Interaction of Human Osteoblasts with Nanostructured Hydroxyapatite (HNA)

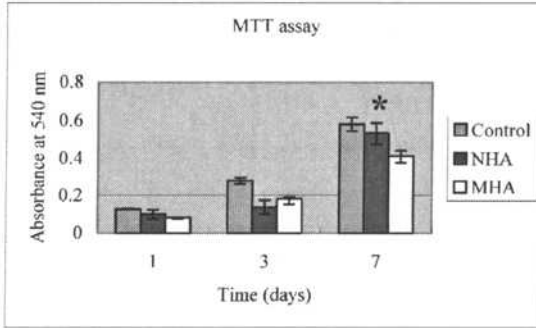


Fig 6 Cell viability on the surface of microstructure HA and nanostructured HA after 1,3,7 days incubation by Alamar Blue assay, control is tissue culture polystyrene

In order to study the long-term cell response, cell proliferation on various samples was measured by Alamar blue assay and MTT assay, which are presented at Fig. 6 and Fig.7, respectively. Both figures showed a similar trend that cell proliferation increased significantly ( $p < 0.05$ ,  $n=3$ ) on both NHA and MHA from 1 day to 7 days. According to Alamar blue assay results, there was no significantly difference between each sample irrespective culture time. However, according to MTT results, cell proliferation was significantly higher on NHA compared to MHA ( $p < 0.05$ ,  $n=3$ ) after 7 days incubation, though there was no significant difference between both surfaces after 1 day and 3 days incubation.

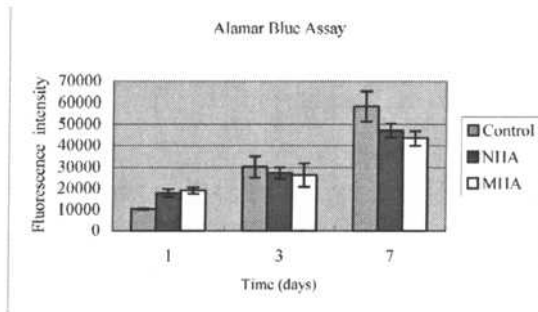


Fig.7 Osteoblasts proliferation on the surface of nanostructured HA and microstructured HA after 1,3,7days in culture. \* Significant from microstructured HA, ( $p < 0.05$ ,  $n=3$ ), control is tissue culture polystyrene

The ability of calcium-containing mineral deposition in extracellular matrix is essential for bone regeneration. The amount of calcium-containing mineral deposited onto the matrix has been quantified by alizarin red stain followed by CPC extraction, results of which are shown in Fig. 8. From 7 days to 14 days incubation, the amount of calcium-containing mineral on NHA surfaces and control increased significantly ( $p < 0.05$ ), but increase slowly on MHA surface.

Furthermore, the amount of calcium-containing mineral on NHA was significantly higher ( $p < 0.05$ ,  $n=3$ ) compared to MHA after 14 days incubation.

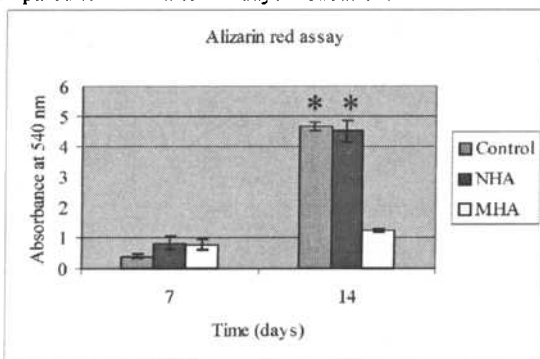


Fig.8 Quantification of alizarin red stain via extraction with 10% CPC in 10mM phosphate buffer on the surface of nanostructured HA and microstructured HA after 14 days in culture. \* Significant from microstructure HA ( $p < 0.05$ ,  $n=3$ ), control is tissue culture polystyrene

#### 4. DISCUSSION

Nanostructured ceramics with grain size less than 100 nm have been widely studied these years due to enhanced magnetic, catalytic, electrical, and optical properties when compared to conventional formulations of the same materials<sup>5</sup>. Nanostructured materials also provide the capability for specific interactions with proteins, DNA, viruses, and other nanoscales biological structures. Highly specific interactions between these components and nanostructured materials can provide unique biological functionalities not seen with conventional microstructured materials<sup>20</sup>. In the present work, we examined the effect of grain size (nano-size, and micro-size) of HA on cellular adhesion, proliferation, and matrix mineralisation. The cell culture system used was human osteoblast.

Cells in contact with a surface will firstly attach, adhere and spread. This first phase of cell adhesion and spreading is known to affect the long-term phenotype of anchorage dependent cells<sup>2, 14</sup>. Osteoblasts, for example, are well documented in the literature, and it can be seen that on some surfaces they appear extremely flattened and on other surfaces they have a more three-dimensional morphology<sup>21</sup>. In this study, the cell morphology for both NHA and MHA as shown by SEM is three-dimensional, while quite flat for glass control. Cells on NHA surface presented more 'spiky' or stellate appearance than that on MHA surface, since more filopodia or microspikes have been observed on NHA surface. The filopodia or microspikes of cells are used in sensing the substrate. Microspikes of neurons extend over significant distances to determine areas suitable for attachment<sup>22</sup>. Therefore, the roughened surface in this study, i.e. NHA surface appears a greater surface area of the cell can adhere. Gough et.al<sup>14</sup> and Dalby et al<sup>23</sup> have observed similar morphologies of osteoblasts cultured on 45S5 bioactive glass and HAPEx<sup>TM</sup> (a composite of hydroxyapatite and polyethylene) with various roughened topography, respectively.

Cell adhesion was also quantified in this study by counting the cell density on various surfaces after 90 min incubation, the results of which show a significant increase of cell adhesion on NHA surface compared to MHA surface and Glass control. Such increased cell adhesion is in

agreement with the more spiky morphology of osteoblasts on NHA surface. It has been previously found that the cell adhesion and spreading are influenced by the physico-chemical characteristics of the underlying solid surface, such as surface free energy of the substrate, surface charge, and surface topography of the biomaterials<sup>24</sup>. In addition, Thomas Webster et.al also found that osteoblast adhesion increased with grain size of ceramics decreasing to nano scale<sup>11</sup>. A possible explanation for such phenomena they suggested could be directly related to the greater surface area exhibited by NHA. The nanostructured surface might promote interaction (such as adsorption, configuration, bioactivity, etc.) of select serum protein(s), which subsequently, enhance osteoblast adhesion<sup>11</sup>. Proteins mediate adhesion of anchorage-dependant cells, and thus influence subsequent cellular functions (such as cell proliferation, matrix mineralisation etc.). The mechanism of protein interaction with nanostructured ceramic is not clear and needs to be further investigated.

Furthermore the average area of spread cell on NHA is significantly lower than that on MHA and Glass control materials. Similar results have been reported by Thomas Webster et.al.<sup>10</sup>, which he suggested might be attributed to the motility of cells. The dynamics of cell migration require continuous forming and breaking of focal contacts at the proximal and distal sides of the cell, respectively. Cell migration is inhibited on substrate surfaces that promote cell adhesion; in other words, contractile forces necessary for cell migration cannot overcome the strength of cell contact points formed on highly adhesive substrate surfaces<sup>25, 26</sup>. Surface occupancy experiments have been utilized as an index of cell population motility<sup>27</sup>. The increased cell adhesion couples with decreased cell motility, as well as enhanced proliferation and matrix mineralisation has been observed on surface (for example, borosilicate glass and titanium) modified with immobilized peptide sequences (such as arginine-glycine-aspartic acid-serine (RGDS) and lysine-arginine-serine-arginine (KRSR)<sup>28-30</sup>) contained in extracellular matrix protein such as vitronectin and collagen.

Matrix mineralisation plays a critical role for the bonding (i.e. osseointegration) between biomaterials and natural bone and bone remodelling. Mineralisation on NHA was significantly greater ( $p < 0.05$ ) than that on MHA after 14 days culture in vitro, which indicates that NHA may greatly enhance osseointegration compared to microstructured HA, and subsequently promote the life span of the implant. The reason for this is not clear yet, however, the more spiky morphology may promote faster matrix production and subsequent mineralisation. It is generally thought that a roughened surface is preferential to strong bone bonding at the tissue-implant interface<sup>14, 31</sup>. In addition, it has been reported that spark plasma sintering<sup>32</sup> also affect the cellular responses; and the presence of soluble calcium phosphate of the MHA will also impact cell proliferation and differentiation<sup>33</sup>. Therefore, further studies are needed to separate the sintering effect and impurity phase effect by fabricating both NHA and MHA structure by SPS process.

## 5. CONCLUSION

In vitro cell culture showed that HOBs attached the surface of NHA with a lot of filopodia after 90min incubate, cell density on NHA surface is significantly higher than that of MHA surface and Glass control after 90 min incubation, whereas the average area of a spread cell after 4 h incubation is significantly lower on NHA surface than that on MHA surface and glass control, which might be attributed to the higher roughness, surface area and wettability of NHA surface, since such difference will affect the protein adsorption on the surface. After 14 days culture, NHA showed a significant enhancement ( $p < 0.05$ ) in matrix mineralisation

compared to MHA. In general, NHA will not only promote the first stage of cell attachment, adhesion and spreading, but also improve the long-term cell proliferation and differentiation.

#### Acknowledgements

This work was partially supported by the Swedish research Council through grant 621-2005-6290.

#### REFERENCE

- <sup>1</sup>Deligianni, D. D., Katsala, N. D., Koutsoukos, P. G., and Missirlis, Y. F., Effect of surface roughness of hydroxyapatite on human bone marrow cell adhesion, proliferation, differentiate and detachment strength. *Biomaterials*, **22**, 87-96(2001).
- <sup>2</sup>Anselme, K., Osteoblast adhesion on biomaterials. *Biomaterials*, **21**, 667-81(2000).
- <sup>3</sup>Anderson, J. M., Gristina, A. G., Hanson, S. R., Harker, L. A., Johnson, R. J., Merritt, K., Naylor, P. T., and Schoen, F. J., *Chapter 4 Host reactions to biomaterials and their evaluation*. 1996, Academic Press, San Diego.
- <sup>4</sup>Thomas, C. H., McFarland, C. D., Jenkins, M. L., Rezanian, A., and Healy, K. E., The role of vitronectin in the attachment and spatial distribution of bone derived cells on materials with patterned surface chemistry. *J. Biomed. Mat. Res.*, **37**, 81-93(1997).
- <sup>5</sup>Webster, T. J., Nanophase ceramics: the future orthopedic and dental implant materials. *Advances in chemical engineering*, **27**, 125-66(2000).
- <sup>6</sup>Barrere, F., Snel, M. M. E., van Blitterswijk, C. A., de Groot, K., and Layrolle, P., Nano-scale study of the nucleation and growth of calcium phosphate coating on titanium implants. *Biomaterials*, **25**, 2901-10(2004).
- <sup>7</sup>Klabunde, K. J., Stark, J., Koper, O., Mohs, C., Park, D., Decker, S., Jiang, Y., Lagadic, I., and Zhang, D., Nanocrystals as stoichiometric reagents with unique surface chemistry. *J. Phys. Chem.*, **100**(30), 12142-53(1996).
- <sup>8</sup>Damien, C. J., and Parsons, J. R., Bone graft and bone graft substitutes: A review of current technology and applications. *Journal of applied biomaterials*, **2**, 187-208(1991).
- <sup>9</sup>Vallet-Regi, M., and Gonzalez-Calbet, J. M., Calcium phosphate as substitution of bone tissue. *Progress in solid state chemistry*, **32**, 1-31(2004).
- <sup>10</sup>Webster, T. J., Ergun, C., Doremus, R. H., Siegel, R. W., and Bizios, R., Enhanced functions of osteoblasts on nanophase ceramics. *Biomaterials*, **21**(17), 1803-10(2000).
- <sup>11</sup>Webster, T. J., Siegel, R. W., and Bizios, R., Osteoblast adhesion on nanophase ceramics. *Biomaterials*, **20**, 1221-27(1999).
- <sup>12</sup>Panda, R. N., Hsieh, M. F., Chung, R. J., and Chin, T. S., FTIR, XRD, SEM and solid state NMR investigations of carbonate-containing hydroxyapatite nano-particles synthesized by hydroxide-gel technique. *Journal of Physics and chemistry of Solids*, **64**, 193-99(2003).
- <sup>13</sup>Wilson, K., and Goulding, K. H., *A biologist's guide to principles and techniques of practical biochemistry*. 1986, Edward Arnold.
- <sup>14</sup>Gough, J. E., Notingher, I., and Hench, L. L., Osteoblast attachment and mineralized nodule formation on rough and smooth 45S5 bioactive glass monoliths. *J Biomed Mater Res*, **68A**(4), 640-50(2004).
- <sup>15</sup>Mosmann, T., Rapid colorimetric assay for cellular growth and survival: application to proliferation and cytotoxicity assays. *J Immunol Methods*, **65**(1-2), 55-63(1983).

- <sup>16</sup>Gloeckner, H., Jonuleit, T., and Lemke, H.-D., Monitoring of cell viability and cell growth in a hollow-fiber bioreactor by use of the dye Alamar Blue™. *Journal of Immunological Methods*, **252**, 131-38(2001).
- <sup>17</sup>Nakayama, G. R., Caton, M. C., Nova, M. P., and Parandoosh, Z., Assessment of the Alamar blue assay for cellular growth and viability in vitro. *Journal of Immunological Methods*, **204**, 205-08(1997).
- <sup>18</sup>Stanford, C. M., Jacobson, P. A., Eanes, E. D., and Lembke, L. A., Rapidly forming apatite mineral in an osteoblastic cell line. *The journal of biological chemistry*, **270**(16), 9420-28(1995).
- <sup>19</sup>Gough, J. E., Jones, J. R., and Hench, L. L., Nodule formation and mineralisation of human primary osteoblasts cultured on a porous bioactive glass scaffold. *Biomaterials*, **25**, 2039-46(2004).
- <sup>20</sup>Narayan, R. J., Kumta, P. N., Sfeir, C., Lee, D.-H., Olton, D., and Choi, D., Nanostructured ceramics in medical devices: Applications and prospects. *JOM*, **56**(10), 38-43(2004).
- <sup>21</sup>Gough, J. E., Schotchford, C. A., and Downes, S., Cytotoxicity of glutaraldehyde crosslinked collagen/poly (vinyl alcohol) films is by the mechanism of apoptosis. *J. Biomed Mater Res*, **61**, 121-30(2002).
- <sup>22</sup>Hammarback, J. A., McCarthy, J. B., Palm, S. L., Furcht, L. T., and Letourneau, P. C., Growth cone guidance by substrate bound laminin pathways is correlated to neuron-to-pathway adhesivity. *Dev Biol*, **126**, 29-39(1988).
- <sup>23</sup>Dalby, M. J., Di-Silvio, L., Gurav, N., Annaz, B., Kayser, M. W., and Bonfield, W., Optimizing HAPEX™ topography influences osteoblast response. *Tissue Eng*, **8**, 453-67(2002).
- <sup>24</sup>Schakenraad, J. M., Cells: Their surfaces and interactions with materials, in *Biomaterials Science: an introduction to materials in medicine*. 1996, Ratner, B. D., Hoffman, A. S., Schoen, F. J., and Lemons, J. E., Eds., Academic Press, London.
- <sup>25</sup>Dickenson, R. B., and Tranquillo, R. T., A stochastic model for adhesion-mediated cell random motility and haptotaxis. *J. Math Biol*, **31**, 563-600(1993).
- <sup>26</sup>Lauffenburger, D. A., Models for receptor-mediated cell phenomena: adhesion and migration. *Ann. Rev. Biophys Chem*, **20**, 387-414(1991).
- <sup>27</sup>Olbrich, K. C., Anderson, T. T., Blumenstock, F. A., and Bizios, R., Surface modified with covalently-immobilized adhesive peptides affect fibroblast population motility. *Biomaterials*, **17**, 759-64(1996).
- <sup>28</sup>Healy, K. E., Rezania, A., and Stile, R. A., Designing biomaterials to direct biological responses. *Ann. NY Acad Sci*, **875**, 24-35(1999).
- <sup>29</sup>Bearingger, J. P., Castner, D. G., and Healy, K. E., Biomolecular modification of p(Aam-co-EG/AA) IPNs supports osteoblast adhesion and phenotypic expression. *J. Biomater Sci Polym Ed*, **7**, 652-92(1998).
- <sup>30</sup>Dee, K. C., Anderson, T. T., and Bizios, R., Design and function of novel osteoblast-adhesive peptides for chemical modification of biomaterials. *J Biomed Mater Res*, **40**, 371-77(1998).
- <sup>31</sup>Gray, C., Boyde, A., and Jones, S. J., Topographically induced bone formation in vitro: Implication for bone implants and bone grafts. *Bone*, **18**, 115-23(1996).
- <sup>32</sup>Nakahira, A., Tamai, M., Aritani, H., Nakamura, S., and Yamashita, K., Biocompatibility of dense hydroxyapatite prepared using an SPS process. *J. Biomed Mater Res*, **60**(4), 550-57(2002).

Initial in Vitro Interaction of Human Osteoblasts with Nanostructured Hydroxyapatite (HNA)

<sup>33</sup>Ogata, K., Imazato, S., Ehara, A., Ebisu, S., Kinomoto, Y., Nakano, T., and Umakoshi, Y., Comparison of osteoblast response to hydroxyapatite and hydroxyapatite/soluble calcium phosphate composites. *J. Biomed Mater Res*, **72A**, 127-35(2005).